Research Article

Abhilash Mavinakere Ramesh, Kaushik Pal, Anju Kodandaram, Bangalore Lakshminarayana Manjula, Doddarasinakere Kempaiah Ravishankar, Hittanahallikoppal Gajendramurthy Gowtham, Mahadevamurthy Murali*, Abbas Rahdar*, and George Z. Kyzas*

Antioxidant and photocatalytic properties of zinc oxide nanoparticles phyto-fabricated using the aqueous leaf extract of *Sida acuta*

https://doi.org/10.1515/gps-2022-0075
received March 30, 2022; accepted July 10, 2022

Abstract: Nanoparticles have gained considerable attention during the present millennium due to its unique properties and usage of same in all the scientific fields. The present study was aimed to phyto-fabricate zinc oxide nanoparticles (ZnO NPs) from *Sida acuta* and evaluate its antioxidant and photocatalytic activity against the dye victoria blue (VB). The phyto-fabricated ZnO NPs when subjected for physico-chemical characterization showed an absorbance peak at 373 nm and was spherical in nature. Strong and well-distinguished sharp peaks were noticed in X-ray diffraction analysis with an average size of ~32.82 nm calculated through Scherrer's formula. The size was also authenticated through dynamic light scattering analysis and transmission electron microscopy. The Fourier transform-infrared spectroscopy confirmed that the phyto-constituents of the plant extract served as capping/stabilizing agents during the synthesis of ZnO NPs. The atomic force microscopy studies on morphology and geometrics of the synthesized particles indicated that particles were monodispersed with colour difference. In addition, the surface area of ZnO NPs measured by Braunauer–Emmett–Teller experimental studies for adsorption isotherms was found to be 7.364 $m^2 \cdot g^{-1}$. The antioxidant efficacy of the phyto-fabricated ZnO NPs offered concentration-dependent antioxidant activity with an IC_{50} value of 0.74 $mg \cdot mL^{-1}$. Further, the VB (9 mM) dye degradation studies using the phyto-fabricated ZnO NPs (0.75 $g \cdot L^{-1}$) resulted in dye degradation of 93% at 40 min in natural sunlight. Further, the reuse and recycling of the photocatalyst for dye degradation offered 70.25% dye degradation ability within 40 min exposure to sunlight at the fifth cycle of reusability thereby indicating effective dye degradation ability of the phyto-fabricated ZnO NPs from the aqueous leaf extract of *S. acuta*.

Keywords: antioxidant, photocatalytic, phyto-fabrication, *Sida acuta*, zinc oxide

*** Corresponding author: Mahadevamurthy Murali,** Department of Studies in Botany, University of Mysore, Manasagangotri, Mysore 570 006, Karnataka, India, e-mail: botany.murali@gmail.com, tel: +91-281-2419758
*** Corresponding author: Abbas Rahdar,** Department of Physics, Faculty of Science, University of Zabol, 98613-35856 Zabol, Iran, e-mail: a.rahdar@uoz.ac.ir
*** Corresponding author: George Z. Kyzas,** Department of Chemistry, International Hellenic University, Kavala, Greece, e-mail: kyzas@chem.ihu.gr
Abhilash Mavinakere Ramesh, Anju Kodandaram: Department of Studies in Environmental Science, University of Mysore, Manasagangotri, Mysore 570 006, India
Kaushik Pal: Department of Physics, University Centre for Research and Development, Chandigarh University, Gharuan, Mohali, Punjab 140 413, India
Bangalore Lakshminarayana Manjula: Department of Botany, Sri Jagadguru Renukacharya College of Science, Arts & Commerce, Race Course Road, Bangalore 560 009, Karnataka, India
Doddarasinakere Kempaiah Ravishankar: Department of Chemistry, Sri Mahadeshwara Government First Grade College, Kollegal 571 440, Karnataka, India
Hittanahallikoppal Gajendramurthy Gowtham: Department of PG Studies in Biotechnology, Government Science College (Autonomous), Nrupathunga Road, Bangalore 560 001, Karnataka, India

1 Introduction

Zinc oxide nanoparticles (ZnO NPs) are one of the most commonly used metal NPs and have been shown to have excellent and important biological properties, including antimicrobial, antioxidant, antidiabetic, anticancer, anti-inflammatory, and photocatalytic as well as drug delivery system [1–4]. The plant-mediated synthesis of NPs has many advantages over conventional physico-chemical

approaches and wide range of biological applications [5–7]. Plants have a wide range of genetic variations in biomolecules and metabolites such as proteins, carbohydrates, vitamins, phenols, flavonoids, sterols, alkaloids, and intermediates [8,9]. These plant metabolites have several functional groups such as hydroxyl (OH), carbonyl (C═O), and amine (NH_2) that react with metal ions to reduce their size to the nanoscale. These molecules aid in the reduction of metal ions into NPs and act as capping for NPs, which is critical for their stability and biocompatibility [4].

The higher toxicity of plant-mediated NPs such as copper (Cu), gold (Au), silver (Ag), and other metal oxides to animals and humans is a significant restriction for their usage in the medical fields [10]. However, ZnO is currently affirmed as safe, which outperforms many other metal oxides in terms of biocompatibility and selectivity, and has a wide range of applications in the antimicrobial, antiviral, biomedical, and environmental fields [1]. Because of their low toxicity and size-dependent properties, ZnO NPs have a greater potential for treating infectious diseases in humans and animals [2]. In the literature, it has been reported that the synthesis of ZnO NPs has been performed using different parts of plant extract, including leaves, stem, bark, flower, fruits, seeds, etc. [4]. Recently various reports have also demonstrated several biological activities of ZnO NPs [3,4] and suggested that the medical industry could benefit greatly from plant-mediated ZnO-NP synthesis.

ZnO is one of the best likely used materials for performing photocatalytic task, as a substitute to the extensively used, comparatively expensive titanium dioxide (TiO_2). Even though researchers recognized comparable photocatalytic mechanisms with both ZnO and TiO_2, they showed that ZnO was found to be a better photocatalyst in degrading the herbicide triclopyr, pesticide carbetamide, pulp mill bleaching wastewater, and phenol, 2-phenylphenol [11]. The capacity of some NPs to speed up a certain reaction in combination with light is generally employed for photocatalysis and this effect is used for self-cleaning surfaces. Photocatalytic activity has been broadly established as one of the most advanced oxidation processes for pollutant degradation. Many oxide semiconductors, like ZnO, SnO_2, have been proven as proficient photocatalysts for degradation of dyes and organic pollutants [2,12,13].

Sida acuta Burm. f., is a weed plant that belongs to the family Malvaceae with numerous medicinal potencies. Because of the wide range of phytochemicals, the plant exhibits a variety of medicinal properties, including antimicrobial, antioxidant, cytotoxic, and other properties [14]. Traditionally, the plant is often believed to treat diseases such as fever, headache, and infectious diseases. It is distinct from other species of the genus due to its acute leaf apex shape and different pair of each stipule. Recently, our research team has phyto-fabricated ZnO NPs from leaf extract of *Sida rhombifolia* Linn. to explore their antibacterial, antioxidant, and genotoxic properties [15]. With this knowledge, the phyto-fabrication of ZnO NPs was also prepared from leaf extract of *S. acuta* to study their antioxidant and photocatalytic properties.

2 Experimental

2.1 Plant collections and phyto-fabrication of ZnO NPs

The healthy leaves of *S. acuta* were collected from Mysore, Karnataka, India. The fresh collected leaf material was cleansed to get rid of dust and debris with running water followed by sterile double distilled water (SDW) and blot dried. In 100 mL of SDW, 10 g of leaf material was grounded using a blender and agitated for 2 h using a rotary shaker at 100 rpm for uniform mixture. Later the solution was filtered using Whatman No. 1 filter paper which served as a source of plant extract. For the NP synthesis of ZnO, zinc nitrate hexahydrate – 2 g was introduced to 20 mL of the above extract and boiled at around 60–80°C, which results in nanopaste. Further the nanopaste was placed in a ceramic crucible and calcinated inside a furnace for 2 h at 300°C. The final product was ZnO NPs in powder form and used for further experimentation [15].

2.2 Characterization of phyto-fabricated ZnO NPs

The UV-visible (UV-Vis) analysis of the phyto-fabricated ZnO NPs was carried out on spectrophotometer (DU730, Beckman Coulter, Krefeld, Germany). X-ray diffraction (XRD) wide-angle patterns were assessed by RIGAKU, Ultima-III Series, Japan. Fourier-transformed infrared (FT-IR) spectra were attained by Thermo Scientific Nicolet, 6700 Analytical FT-IR Spectrometers (FLS-1000). The morphology of the phyto-fabricated ZnO was studied by FE-SEM, HITACHI (Noran System 7, USA) along with detection of metals through energy dispersive X-ray (EDX) analysis (Zeiss Supra 55VP, Japan). To determine the size of the ZnO NPs high-resolution-transmission electron microscopy (HR-TEM) examination

was performed using Jeol/JEM-2100 (Japan) instrument. Particle size analyser (Microtrac, USA) was designated to evaluate the phyto-fabricated ZnO for particle size distribution (PDS). The synthesized particles were also subjected to atomic force microscopy (AFM 100, Italy) for the surface morphology and particle size variation. The Braunauer–Emmett–Teller (BET) aids in the efficient measuring of the specific surface area, pore size, pore volume, and their distribution using BEL:2 SORP, Italy.

2.3 Antioxidant activity of phyto-fabricated ZnO NPs

The radical scavenging activity (RSA) of phyto-fabricated ZnO NPs was performed by 2,2-diphenyl-1-picrylhydrazyl (DPPH) method [16]. In brief, to 3.5 mL of 0.1 mM DPPH containing different concentrations of NPs (0–1 mg·mL^{-1}) were subjected to sonication before incubation at 37 ± 2°C for 30 min under dark conditions. The absorbance of the incubated samples was read at 517 nm in a spectrophotometer and percent RSA was determined:

$$\text{Radical scavenging activity (\%)} = \frac{\text{Absorbance of control} - \text{Absorbance of test sample}}{\text{Absorbance of control}} \times 100 \quad (1)$$

2.4 Photocatalytic activity

The photocatalytic degradation of victoria blue (VB) dye using phyto-fabricated ZnO NPs was evaluated under solar irradiation of 430–770 THz. Approximately, 0.75 g·L^{-1} of catalyst was allowed to react with VB of 9 mM concentration initially in a flask. The experiment was conducted upon various pH concentrations from 2 to 7. The flasks were placed upon the continuous magnetic stirrer under the solar radiation [17]. The level of photocatalyst dye degradation efficiency was evaluated via characteristic absorption peak of 550 nm [18]. A pseudo-first-order kinetic model was used to describe the relationship of adsorption and photo-degradation between solid–liquid systems. The experimental values were fitted with the rate equation:

$$-\ln(C_t/C_0) = k(p) \times t \quad (2)$$

where C_t is the absorbance of VB at t time, C_0 is the absorbance of VB after dark adsorption, t is the irradiation time, and $k(p)$ is the pragmatic kinetic constant. The pseudo-first-order rate constant, kp (min^{-1}), was calculated from the slope of $\ln(C_t/C_0)$ versus irradiation time (t).

2.5 Statistical analysis

Every attempt of analysis was made in triplicates for accurate results using SPSS-Inc. 16.0 (ANOVA). Trivial effects of treatments were resolved by F values ($p \leq 0.05$).

3 Results and discussion

3.1 Characterization of phyto-fabricated ZnO NPs

The UV-Vis spectral analysis of the phyto-fabricated ZnO NPs revealed a peak at 373 nm (Figure 1), which is in line with the results of the previous studies wherein a peak was observed between 315 and 400 nm that is characteristic of Zn [5,8]. The XRD analysis was performed to additional phase confirmation of the phyto-fabricated ZnO. XRD peaks are well indexed with JCPDS No. 89-510 (Joint Committee on Powder Diffraction Standards 01-079-0207) corresponding to (100), (002), (101), (102), (110), (103), (200), (112), (201), and (202) planes, angles of 31.76°, 34.47°, 36.24°, 47.54°, 56.61°, 62.83°, 66.45°, 67.90°, 69.06°, and 77.02° were resulted, respectively (Figure 2). The size of the ZnO NPs calculated using Scherrer's formula showed the average particle size of ~32.82 nm. The strong and well-distinguished sharp peaks depicted particle morphology with well-outlined crystallinity [19,20]. The FT-IR spectrum of the phyto-fabricated ZnO NPs and plant extract was recorded in the 400–4,000 cm^{-1} range (Figure 3 and Table A1 in Appendix). The spectral analysis helps in identifying the

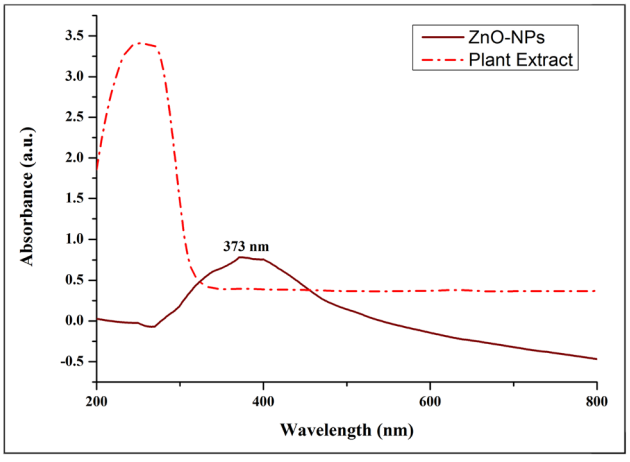

Figure 1: UV-Vis spectroscopic analysis of phyto-fabricated ZnO from *S. acuta*.

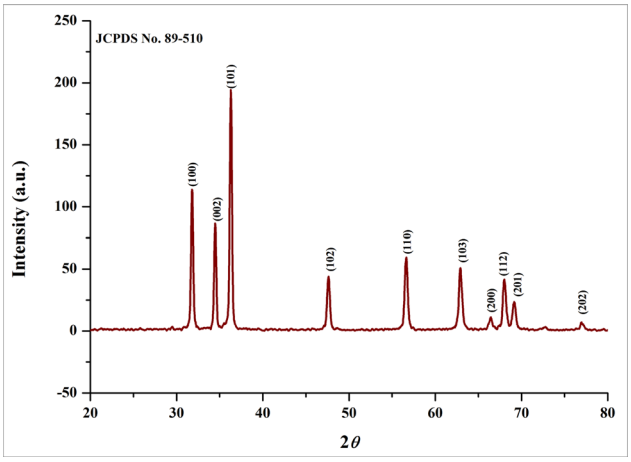

Figure 2: XRD profile of phyto-fabricated ZnO NPs from *S. acuta*.

functional groups of the plant extract that are involved during reduction and stabilization of plant extracts during phyto-fabrication [8]. From the study it was noted that, absence of peaks around 3,250 cm^{-1} and the presence of same in plant extract indicated the particles were free from moisture. In addition, peak noticed at the 544 cm^{-1} in the phyto-fabricated ZnO NPs corresponds to Zn–O bond (metal oxide) as indicated by Yuvakkumar et al. [21] and Bhuyan et al. [22]. From the results of the FT-IR, it is noted that during the formation of ZnO NPs, zinc ions (Zn^{2+}) will cap with the available phyto-constituents of the plant extract to form a complex compound which undergoes direct decomposition at 300°C in static air atmosphere finally leading in the formation of ZnO NPs (Figure 4) which is in accordance with the previous studies [23,24]. In addition it has been reported that during the synthesis of the ZnO NPs the phyto-constituents (primary, secondary, or tertiary metabolites) act as capping,

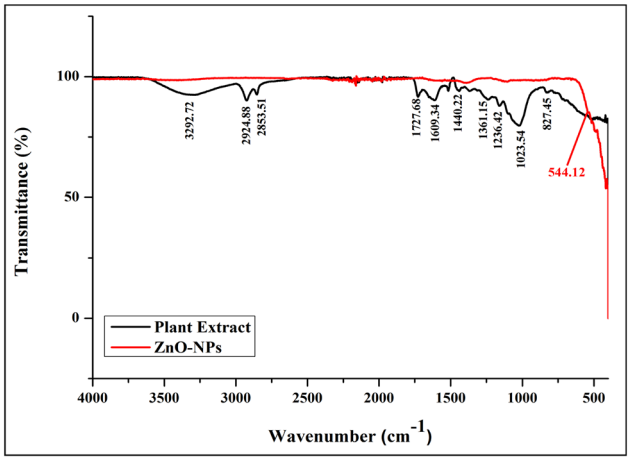

Figure 3: FT-IR spectrum of phyto-fabricated ZnO NPs from *S. acuta*.

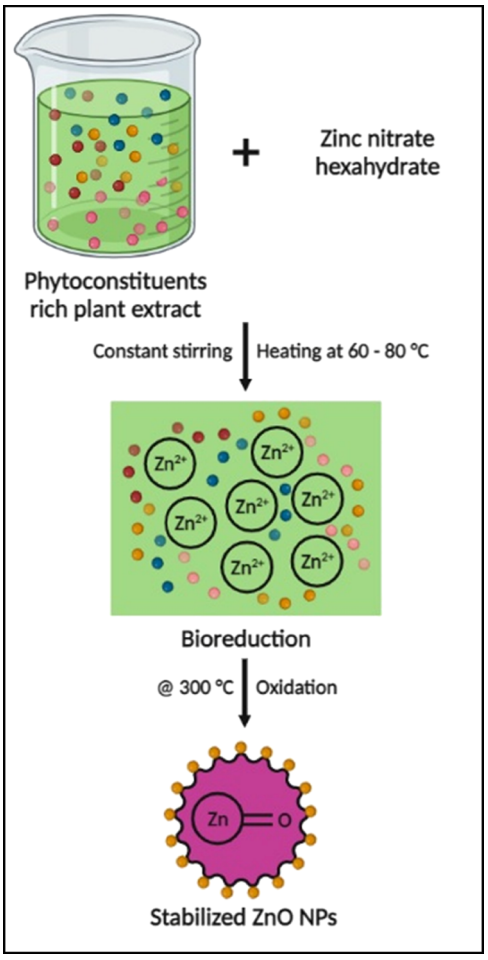

Figure 4: Plausible mechanism involved during the formation of ZnO NPs from the aqueous extract of *S. acuta*.

reducing, and stabilizing agents [25–28]. The FE-SEM results of the NPs showed that the particles were agglomerated (Figure 5). Similarly, the quantitative elemental analysis using EDX analysis revealed the presence of zinc (53.88%),

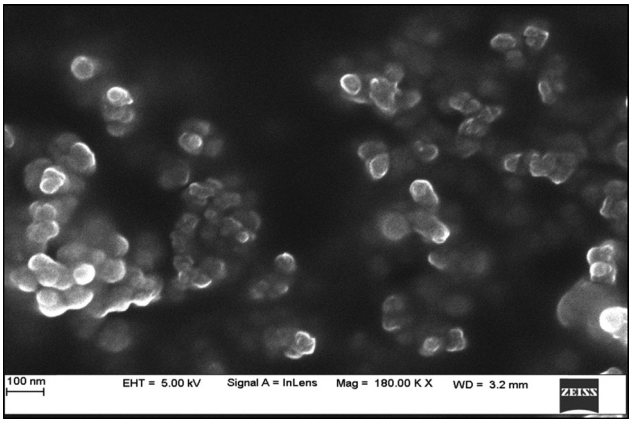

Figure 5: FE-SEM of phyto-fabricated ZnO NPs from *S. acuta*.

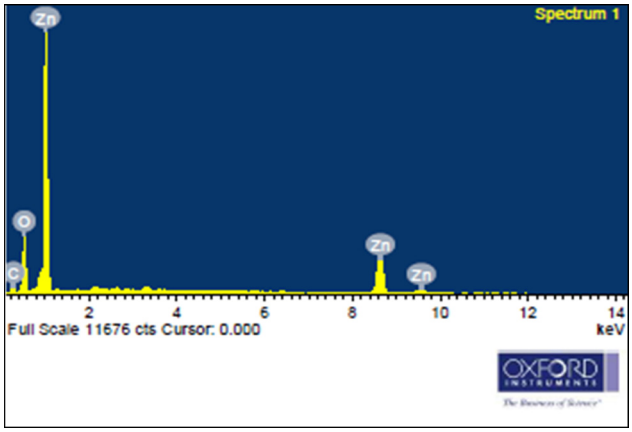

Figure 6: Elemental composition of phyto-fabricated ZnO NPs from *S. acuta*.

oxygen (32.30%), and traces of carbon (Figure 6). The TEM analysis of the phyto-fabricated ZnO NPs confirmed the nanorange in size (Figure 7a), while the selected area electron diffraction (SAED) is shown in Figure 7b, which confirmed the polycrystallinity nature of the particles. In addition, the XRD peaks (Miller indices) matched well with the SAED pattern of the particles and the estimated *d*-spacing value of the same was found to be 0.32 nm which confirmed clear separation of the inter-planar spacing (Figure 7c). Further, the dynamic light scattering (DLS) histogram obtained from the PDS demonstrated that the particles were of the average diameter of ~44.5 nm (Figure 8) which was in agreement with the findings of Rouhi et al. [29]. The high-quality images obtained for the particles with AFM are vital for correcting ample background and slope [30,31]. The morphology and geometrics of the phyto-fabricated ZnO NPs were found to be monodispersed. Along with these findings, colour difference due to morphology and particle size variation was also presented by AFM analysis (Figure 9). It has been well documented that the inert nature via high surface area becomes a vital parameter in defining biological adaptability. A larger surface area draws the biological matter rapidly and provides biological systems a well-developed transport lanes and wider surface-active sites for reactant molecules and products. The BET experimental studies for adsorption isotherms were executed at 77.3 K with relative pressure up to P/P_0 ~0.911. According to the hysteresis loop in the

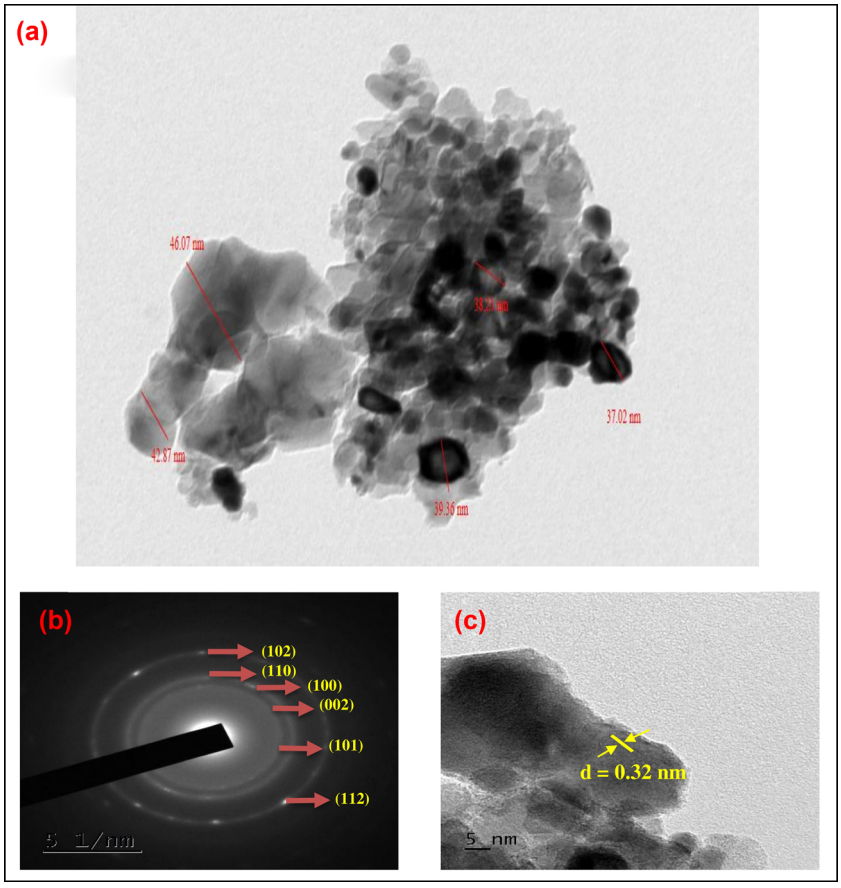

Figure 7: TEM image of phyto-fabricated ZnO NPs from *S. acuta* (a), SAED pattern of ZnO NPs (b), and HR-TEM with *d*-spacing (c).

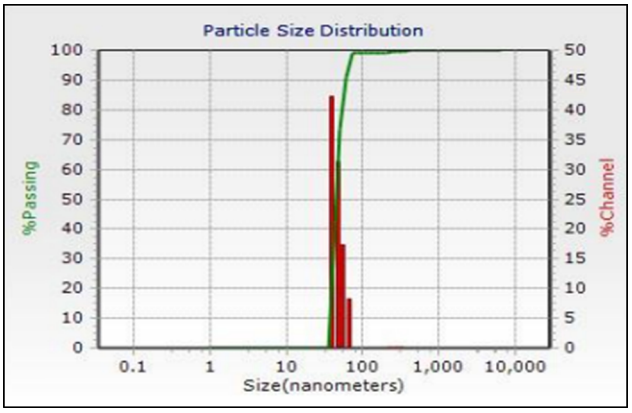

Figure 8: DLS of phyto-fabricated ZnO NPs from *S. acuta*.

relative pressure region of around 0.4–0.9, the nitrogen adsorption/desorption isotherms for the particles are depicted in Figure 8. The observed results demonstrate a type-IV isotherm curve with H-3 hysteresis loop characteristics of mesoporous structure, according to IUPAC classification [21,22]. The surface area of ZnO measured by BET was found to be 7.364 $m^2 \cdot g^{-1}$ which was obtained through BET constant (C) (96.53) thereby indicating that the dye molecules may enter easily into the inner space of NPs and then disperse helping in the photocatalytic properties. Furthermore, the Barrette-Joyner-Halenda method was used to measure the pore size and pore volume distribution in addition to the idea of surface area and its mean pore size diameter is about 5.26 nm (Figure 10) [32].

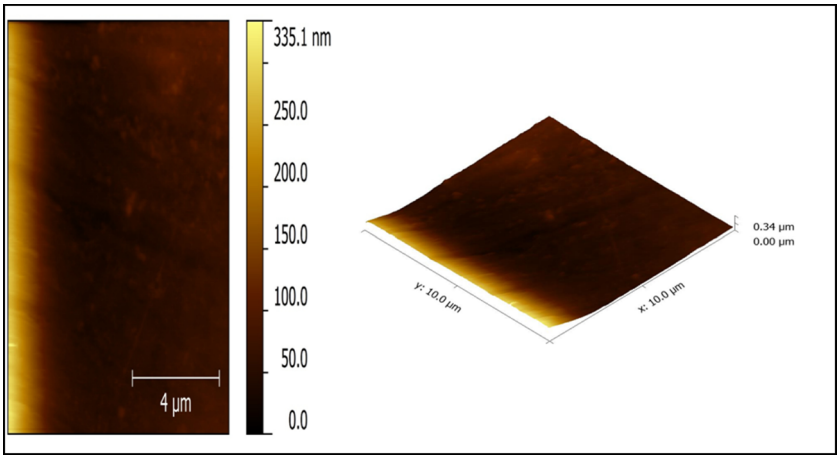

Figure 9: AFM images of phyto-fabricated ZnO NPs from *S. acuta*.

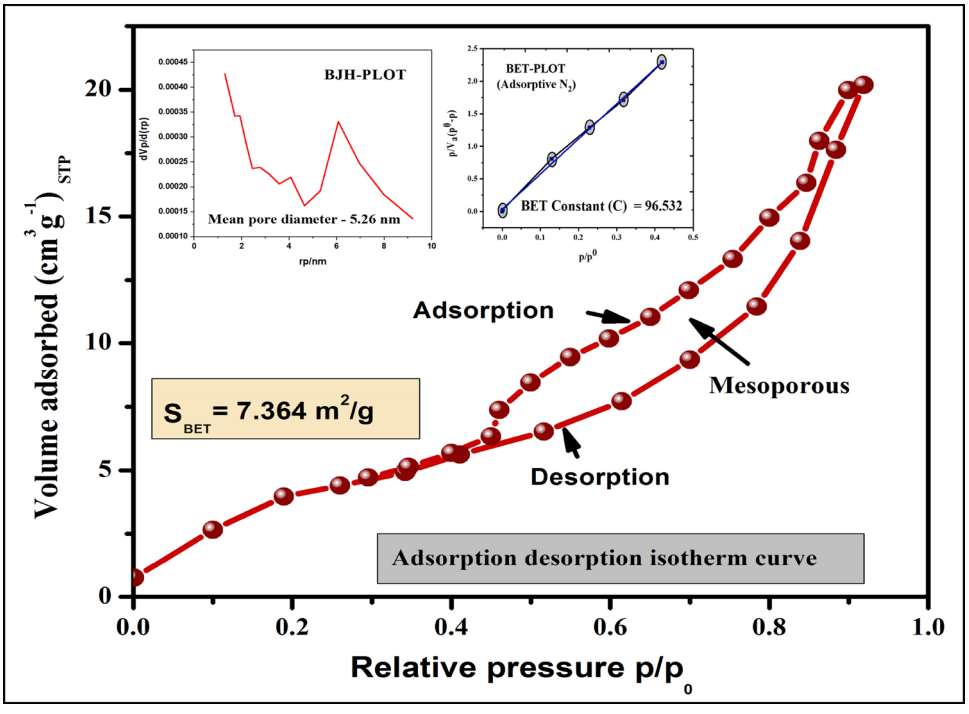

Figure 10: BET and N_2 adsorption isotherms of phyto-fabricated ZnO NPs from *S. acuta*.

3.2 Antioxidant activity

The radical scavenging properties of the phyto-fabricated ZnO NPs evaluated through the DPPH method showed an increased RSA with an increase in the NPs' concentration. The NPs' half-maximal inhibitory concentration (IC_{50}) was found to be 0.74 mg·mL^{-1} (Figure 11). It was also noted that the aqueous plant extract did not offer any antioxidant activity at the above-said concentrations (Table A2), while the positive control ascorbic acid offered more than 75% inhibition at 50 µg·mL^{-1}. The antioxidant potentiality of the phyto-fabricated NPs may be attributed to the capping of phytoconstituents present in the plant extract during the synthesis process [11,33]. In addition, the results are in corroboration with the findings of many studies wherein the plant-mediated synthesis of ZnO NPs showed better antioxidant properties when evaluated through the DPPH method compared to their respective plant extracts [16] and are also known to be more effective than the chemically synthesized NPs [34].

3.3 Photocatalytic activity

The photocatalytic dye degradation efficiency was reflected through the experiments conducted by varying the concentrations of dye and catalysts [32]. Under visible light photocatalysis, the ZnO was relatively stable, whereas the VB dye deteriorated swiftly within 40 min. At 40 min in natural sunlight, the phyto-fabricated ZnO degraded VB up to 93% (0.75 g·L^{-1}) according to this study. It was noted that with the increase in the concentration of the NPs the VB dye degradation ability increased (Figure 12a). In accordance, biosynthesized ZnO NPs have been found to be effective in degrading the dyes more efficiently [35,36]. The photo-

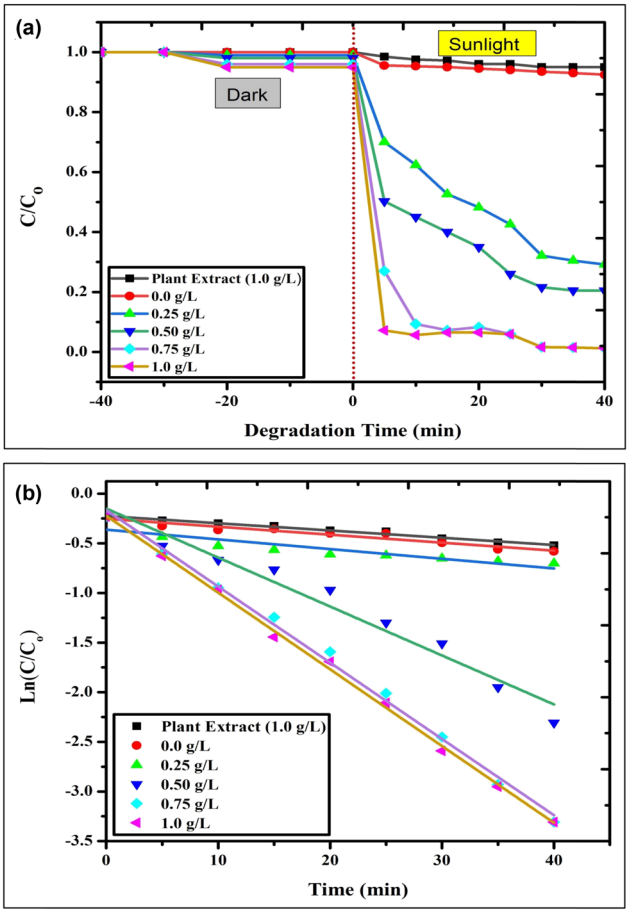

Figure 12: Photo removal (a) and kinetics (b) of phyto-fabricated ZnO NPs from *S. acuta*.

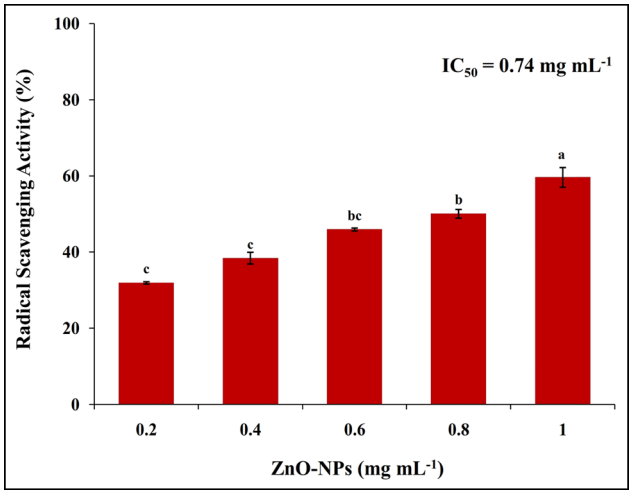

Figure 11: Antioxidant potentiality of phyto-fabricated ZnO NPs from *S. acuta*.

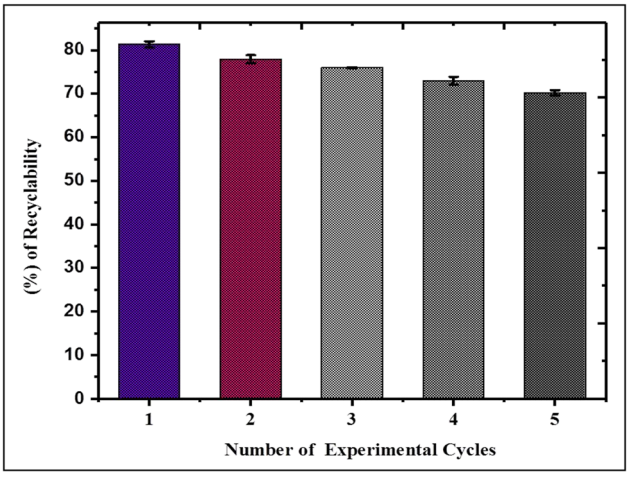

Figure 13: Recycling performance of the photo-removal of phyto-fabricated ZnO NPs from *S. acuta*.

Table 1: Morphology of plant-mediated ZnO NPs and their applications

Plant name	Plant part used	Size (nm)	Shape/morphology	Applications	Reference
Cassia fistula	Leaf	~5–15	Sponge like irregular	Photocatalytic and antioxidant	[40]
Artocarpus gomezianus	Fruit	11.53	Spherical	Photocatalytic and antioxidant	[11]
Azadirachta indica	Leaf	10–30	Hexagonal	Antioxidant and photocatalytic	[41]
Eucalyptus globulus	Leaf	11.6	Spherical	Antioxidant and photocatalytic	[42]
Trianthema portulacastrum	Plant	25–90	Spherical	Antioxidant and photocatalytic	[43]
Mussaenda frondosa	Leaf	8–15	Hexagonal	Antioxidant and photocatalytic	[44]
	Stem	9–12	Spherical		
	Leaf-derived callus	5–7			
Aegle marmelos	Juice	~20	Hexagonal	Antioxidant and photocatalytic	[45]
Sambucus ebulus	Leaf	25–30	Spherical	Antioxidant and photocatalytic	[36]
Syzygium aromaticum	Buds	50	Hexagonal	Antioxidant and photocatalytic	[46]
Myristica fragrans	Fruit	43–83	Spherical or elliptical	Antioxidant and photocatalytic	[37]
S. acuta	Leaf	~32.82	Spherical	Antioxidant and photocatalytic	Present study

degradation reactions for VB exhibit pseudo-first-order kinetics and kinetics was well explained using the model [37]. The photocatalytic removal of VB follows the pragmatic rate constant for ZnO of $0.425 \times 10^{-2}\,s^{-1}$ (Figure 12b). The degradation of VB by the phyto-fabricated ZnO NPs exhibited relatively fast kinetics with a rate constant of $k = 0.425\,min^{-1}$.

3.4 Recyclability of phyto-fabricated ZnO

In order to reduce the stress upon the raw material of phyto-fabricated ZnO photocatalyst, reuse and recycling of the photocatalyst were attempted. The nanocatalyst recovered after dye degradation was washed using deionized water and ethanol, followed by drying and reused for the next cycle. A total of five trials of dye degradation were experimented using the same photocatalyst from the first to the fifth cycle, the percentage VB dye degradation efficiency using phyto-fabricated ZnO NPs was found to be 81.36%, 77.98%, 75.99%, 73.01%, and 70.25%, respectively, within 40 min with sunlight influence (Figure 13). The results of the study indicated remarkable photostability. As compared to the chemically synthesized nanomaterials, phyto-encapsulated ZnO NPs have the equivalent recyclable efficiency [38,39] and also the synthesized NPs being a plant extract makes it ecological and environmental friendly material. Due to the efficient recyclable property of the photocatalyst there will be fewer requirements for the production of new photocatalyst, and it is cost effective. Also the photocatalyst can be reused even for more than five cycles only with lesser degradation percentage. These give the photocatalyst the positive remarks.

In addition, Table 1 shows the importance of phyto-fabricated ZnO NPs and their antioxidant and photocatalytic applicability. The table represents the plant and its part used, size, morphology, and application of ZnO NPs and the results of the present study are also compared.

4 Conclusions

The present study is the first report on the phyto-fabrication of ZnO NPs from *S. acuta*. The phyto-fabricated NPs were of ~32.82 nm calculated through Scherrer's formula. The UV-Vis spectra and FT-IR analysis of the particles showed a characteristic peaks at 373 nm and 544.12 cm^{-1}, which are correlated to Zn and metal oxide bond, respectively. The surface area of ZnO measured by BET was found to be 7.364 $m^2 \cdot g^{-1}$. The antioxidant studies revealed the phyto-fabricated particles possessed RSA which was concentration dependent with an IC_{50} value of 0.74 $mg \cdot mL^{-1}$. The dye degradation studies of the particles against the VB showed 93% degradation of the dye after 40 min exposure to natural sunlight. In addition, the reuse and recycling of the photocatalyst for dye degradation offered 70.25% degradation ability at the fifth cycle of reuse thereby signifying the dye degradation ability of the phyto-fabricated ZnO NPs.

Acknowledgment: The authors thank the Department of Studies in Environmental Science, Botany, and Biotechnology, University of Mysore, India for providing the necessary facility to carry out the research work.

Funding information: Authors state no funding involved.

Author contributions: Abhilash Mavinakere Ramesh, Kaushik Pal, Anju Kodandaram, and Mahadevamurthy Murali: methodology; Bangalore Lakshminarayana Manjula, Doddarasinakere Kempaiah Ravishankar, and Kaushik Pal: formal analysis; Bangalore Lakshminarayana Manjula, Doddarasinakere Kempaiah Ravishankar, Hittanahallikoppal Gajendramurthy Gowtham, and Kaushik Pal: visualization; Abhilash Mavinakere Ramesh, Mahadevamurthy Murali, and Abbas Rahdar: writing – original draft; Abhilash Mavinakere Ramesh, Mahadevamurthy Murali, Abbas Rahdar, and George Z. Kyzas: resources; Mahadevamurthy Murali, Abbas Rahdar, and George Z. Kyzas: project administration. All the authors equally contributed for writing – review and editing and approved the final manuscript.

Conflict of interest: Authors state no conflict of interest.

Data availability statement: Available data are presented in the manuscript.

References

[1] Saemi R, Taghavi E, Jafarizadeh-Malmiri H, Anarjan N. Fabrication of green ZnO nanoparticles using walnut leaf extract to develop an antibacterial film based on polyethylene–starch–ZnO NPs. Green Process Synth. 2021;10(1):112–24. doi: 10.1515/gps-2021-0011.

[2] Vahidi A, Vaghari H, Najian Y, Najian MJ, Jafarizadeh-Malmiri H. Evaluation of three different green fabrication methods for the synthesis of crystalline ZnO nanoparticles using *Pelargonium zonale* leaf extract. Green Process Synth. 2019;8(1):302–8. doi: 10.1515/gps-2018-0097.

[3] Chunchegowda UA, Shivaram AB, Mahadevamurthy M, Ramachndrappa LT, Lalitha SG, Krishnappa HKN, et al. Biosynthesis of zinc oxide nanoparticles using leaf extract of *Passiflora subpeltata*: characterization and antibacterial activity against *Escherichia coli* isolated from poultry faeces. J Clust Sci. 2021;32:1663–72. doi: 10.1007/s10876-020-01926-0.

[4] Murali M, Kalegowda N, Gowtham HG, Ansari MA, Alomary MN, Alghamdi S, et al. Plant-mediated zinc oxide nanoparticles: advances in the new millennium towards understanding their therapeutic role in biomedical applications. Pharmaceutics. 2021;13(10):1662. doi: 10.3390/pharmaceutics13101662.

[5] Mahendra C, Chandra MN, Murali M, Abhilash MR, Singh SB, Satish S, et al. Phyto-fabricated ZnO nanoparticles from *Canthium dicoccum* (L.) for antimicrobial, anti-tuberculosis and antioxidant activity. Process Biochem. 2020;89:220–26. doi: 10.1016/j.procbio.2019.10.020.

[6] Buazar F. Impact of biocompatible nanosilica on green stabilization of subgrade soil. Sci Rep. 2019;9:15147. doi: 10.1038/s41598-019-51663-2.

[7] Moavi J, Buazar F, Sayahi MH. Algal magnetic nickel oxide nanocatalyst in accelerated synthesis of pyridopyrimidine derivatives. Sci Rep. 2021;11:1–14. doi: 10.1038/s41598-021-85832-z.

[8] Murali M, Mahendra C, Nagabhushan, Rajashekar N, Sudarshana MS, Raveesha KA, et al. Antibacterial and antioxidant properties of biosynthesized zinc oxide nanoparticles from *Ceropegia candelabrum* L. – an endemic species. Spectrochim Acta A Mol Biomol Spectrosc. 2017;179:104–9. doi: 10.1016/j.saa.2017.02.027.

[9] Murali M, Manjula S, Shilpa N, Ravishankar DK, Shivakumar CS, Thampy A, et al. Facile synthesis of ZnO-NPs from yellow creeping daisy (*Sphagneticola trilobata* L.) attenuates cell proliferation by inducing cellular level apoptosis against colon cancer. J King Saud Univ Sci. 2022;34(5):102084. doi: 10.1016/j.jksus.2022.102084.

[10] Das RK, Pachapur VL, Lonappan L, Naghdi M, Pulicharla R, Maiti S, et al. Biological synthesis of metallic nanoparticles: plants, animals and microbial aspects. Nanotechnol Environ Eng. 2017;2:18. doi: 10.1007/s41204-017-0029-4.

[11] Suresh D, Shobharani RM, Nethravathi PC, Pavan Kumar MA, Nagabhushana H, Sharma SC. *Artocarpus gomezianus* aided green synthesis of ZnO nanoparticles: luminescence, photocatalytic and antioxidant properties. Spectrochim Acta A Mol Biomol Spectrosc. 2015;141:128–34. doi: 10.1016/j.saa.2015.01.048.

[12] Uddin MT, Nicolas Y, Olivier C, Toupance T, Servant L, Müller MM, et al. Nanostructured SnO_2–ZnO heterojunction photocatalysts showing enhanced photocatalytic activity for the degradation of organic dyes. Inorg Chem. 2012;51(14):7764–73. doi: 10.1021/ic300794j.

[13] Luque-Morales PA, Lopez-Peraza A, Nava-Olivas OJ, Amaya-Parra G, Baez-Lopez YA, Orozco-Carmona VM, et al. ZnO semiconductor nanoparticles and their application in photocatalytic degradation of various organic dyes. Materials. 2021;14(24):7537. doi: 10.3390/ma14247537.

[14] Simplice DK, Wendyam MN, Denise PI, Djeneba O, Messanvi G, Comlan DS, et al. *Sida acuta* Burm. f.: a medicinal plant with numerous potencies. Afr J Biotechnol. 2007;6(25):2953–59. doi: 10.5897/AJB2007.000-2463.

[15] Kavya JB, Murali M, Manjula S, Basavaraj GL, Prathibha M, Jayaramu SC, et al. Genotoxic and antibacterial nature of biofabricated zinc oxide nanoparticles from *Sida rhombifolia* Linn. J Drug Deliv Sci Technol. 2020;60:101982. doi: 10.1016/j.jddst.2020.101982.

[16] Hemanth Kumar NK, Murali M, Satish A, Brijesh Singh S, Gowtham HG, Mahesh HM, et al. Bioactive and biocompatible nature of green synthesized zinc oxide nanoparticles from *Simarouba glauca* DC.: an endemic plant to Western Ghats, India. J Clust Sci. 2020;31:523–34. doi: 10.1007/s10876-019-01669-7.

[17] Chakrabarti S, Dutta BK. Photocatalytic degradation of model textile dyes in wastewater using ZnO as semiconductor catalyst. J Hazard Mater. 2004;112(3):269–78. doi: 10.1016/j.jhazmat.2004.05.013.

[18] Yang L, Guan X, Wang GS, Guan XH, Jia B. Synthesis of ZnS/CuS nanospheres loaded on reduced graphene oxide as high-performance photocatalysts under simulated sunlight irradiation. N J Chem. 2017;41(13):5732–44. doi: 10.1039/C7NJ00801E.

[19] Srivastava V, Gusain D, Sharma YC. Synthesis, characterization and application of zinc oxide nanoparticles (n-ZnO). Ceram Int. 2013;39(8):9803–08. doi: 10.1016/j.ceramint.2013.04.110.

[20] Vergés MA, Mifsud A, Serna C. Formation of rod-like zinc oxide microcrystals in homogeneous solutions. J Chem Soc Faraday Trans. 1990;86(6):959–63. doi: 10.1039/FT9908600959.

[21] Yuvakkumar R, Suresh J, Nathanael AJ, Sundrarajan M, Hong SI. Novel green synthetic strategy to prepare ZnO nanocrystals using rambutan (*Nephelium lappaceum* L.) peel extract and its antibacterial applications. Mater Sci Eng C. 2014;41:17–27. doi: 10.1016/j.msec.2014.04.025.
[22] Bhuyan T, Mishra K, Khanuja M, Prasad R, Varma A. Biosynthesis of zinc oxide nanoparticles from *Azadirachta indica* for antibacterial and photocatalytic applications. Mater Sci Semicond Process. 2015;32:55–61. doi: 10.1016/j.mssp.2014.12.053.
[23] Karnan T, Selvakumar SAS. Biosynthesis of ZnO nanoparticles using rambutan (*Nephelium lappaceum* L.) peel extract and their photocatalytic activity on methyl orange dye. J Mol Struct. 2016;1125:358–65. doi: 10.1016/j.molstruc.2016.07.029.
[24] Jafarirad S, Mehrabi M, Divband B, Kosari-Nasab M. Biofabrication of zinc oxide nanoparticles using fruit extract of *Rosa canina* and their toxic potential against bacteria: a mechanistic approach. Mater Sci Eng C Mater Biol Appl. 2016;59:296–302. doi: 10.1016/j.msec.2015.09.089.
[25] Buazar F, Bavi M, Kroushawi F, Halvani M, Khaledi-Nasab A, Hossieni SA. Potato extract as reducing agent and stabiliser in a facile green one-step synthesis of ZnO nanoparticles. J Exp Nanosci. 2016;11(3):175–84. doi: 10.1080/17458080.2015.1039610.
[26] Buazar F, Sweidi S, Badri M, Kroushawi F. Biofabrication of highly pure copper oxide nanoparticles using wheat seed extract and their catalytic activity: a mechanistic approach. Green Process Synth. 2019;8(1):691–702. doi: 10.1515/gps-2019-0040.
[27] Koopi H, Buazar F. A novel one-pot biosynthesis of pure alpha aluminum oxide nanoparticles using the macroalgae *Sargassum ilicifolium*: a green marine approach. Ceram Int. 2018;44(8):8940–5. doi: 10.1016/j.ceramint.2018.02.091.
[28] Sepahvand M, Buazar F, Sayahi MH. Novel marine-based gold nanocatalyst in solvent-free synthesis of polyhydroquinoline derivatives: green and sustainable protocol. Appl Organomet Chem. 2020;34(12):e6000. doi: 10.1002/aoc.6000.
[29] Rouhi J, Mahmud S, Naderi N, Raymond Ooi CH, Mahmood MR. Physical properties of fish gelatin-based bio-nanocomposite films incorporated with ZnO nanorods. Nanoscale Res Lett. 2013;8(1):364. doi: 10.1186/1556-276X-8-364.
[30] Park WI, Yi GC. Schottky nanocontacts on ZnO nanorod arrays. Appl Phys Lett. 2003;82(24):4358–60. doi: 10.1063/1.1584089.
[31] Solís-Pomar F, Martínez E, Meléndrez MF, Pérez-Tijerina E. Growth of vertically aligned ZnO nanorods using textured ZnO films. Nanoscale Res Lett. 2011;6(1):524. doi: 10.1186/1556-276X-6-524.
[32] Rouquerol J, Llewellyn P, Rouquerol F. Is the BET equation applicable to microporous adsorbents. Stud Surf Sci Catal. 2007;160(7):49–56. doi: 10.1016/s0167-2991(07)80008-5.
[33] Venkateasan A, Prabakaran R, Sujatha V. Phytoextract-mediated synthesis of zinc oxide nanoparticles using aqueous leaves extract of *Ipomoea pes-caprae* (L). R. br revealing its biological properties and photocatalytic activity. Nanotechnol Environ Eng. 2017;2:8. doi: 10.1007/s41204-017-0018-7.
[34] Stan M, Popa A, Toloman D, Silipas TD, Vodnar DC. Antibacterial and antioxidant activities of ZnO nanoparticles synthesized using extracts of *Allium sativum, Rosmarinus officinalis* and *Ocimum basilicum*. Acta Met Sin Engl Lett. 2016;29:228–36. doi: 10.1007/s40195-016-0380-7.
[35] Zhang H, Chen B, Jiang H, Wang C, Wang H, Wang X. A strategy for ZnO nanorod mediated multi-mode cancer treatment. Biomaterials. 2011;32(7):1906–14. doi: 10.1016/j.biomaterials.2010.11.027.
[36] Alamdari S, Ghamsari MS, Lee C, Han W, Park HH, Tafreshi MJ, et al. Preparation and characterization of zinc oxide nanoparticles using leaf extract of *Sambucus ebulus*. Appl Sci. 2020;10:3620. doi: 10.3390/app10103620.
[37] Faisal S, Jan H, Shah SA, Shah S, Khan A, Akbar MT, et al. Green synthesis of zinc oxide (ZnO) nanoparticles using aqueous fruit extracts of *Myristica fragrans*: their characterizations and biological and environmental applications. ACS Omega. 2021;6:9709–22. doi: 10.1021/acsomega.1c00310.
[38] Meng ZD, Zhu L, Choi JG, Park CY, Oh WC. Preparation, characterization and photocatalytic behavior of WO_3-fullerene/TiO_2 catalysts under visible light. Nanoscale Res Lett. 2011;6:459. doi: 10.1186/1556-276X-6-459.
[39] Seger B, Laursen AB, Vesborg PC, Pedersen T, Hansen O, Dahl S, et al. Hydrogen production using a molybdenum sulfide catalyst on a titanium-protected n^+p-silicon photocathode. Angew Chem Int Ed Engl. 2012;51:9128–31. doi: 10.1002/anie.201203585.
[40] Suresh D, Nethravathi PC, Udayabhanu, Rajanaika H, Nagabhushana H, Sharma SC. Green synthesis of multifunctional zinc oxide (ZnO) nanoparticles using *Cassia fistula* plant extract and their photodegradative, antioxidant and antibacterial activities. Mater Sci Semicond Process. 2015;31:446–54. doi: 10.1016/j.mssp.2014.12.023.
[41] Madan HR, Sharma SC, Rajanaik H, Suresh D, Vidya YS, Nagabhushana H, et al. Facile green fabrication of nanostructure ZnO plates, bullets, flower, prismatic tip, closed pine cone: their antibacterial, antioxidant, photoluminescent and photocatalytic properties. Spectrochim Acta A Mol Biomol Spectrosc. 2016;152:404–16. doi: 10.1016/j.saa.2015.07.067.
[42] Siripireddy B, Mandal BK. Facile green synthesis of zinc oxide nanoparticles by *Eucalyptus globulus* and their photocatalytic and antioxidant activity. Adv Powder Technol. 2017;28:785–97. doi: 10.1016/j.apt.2016.11.026.
[43] Khan ZUH, Sadiq HM, Shah NS, Khan AU, Muhammad N, Hassan SU, et al. Greener synthesis of zinc oxide nanoparticles using *Trianthema portulacastrum* extract and evaluation of its photocatalytic and biological applications. J Photochem Photobiol B Biol. 2019;192:147–57. doi: 10.1016/j.jphotobiol.2019.01.013.
[44] Jayappa MD, Ramaiah CK, Kumar MAP, Suresh D, Prabhu A, Devasya RP, et al. Green synthesis of zinc oxide nanoparticles from the leaf, stem and *in vitro* grown callus of *Mussaenda frondosa* L.: characterization and their applications. Appl Nanosci. 2020;10:3057–74. doi: 10.1007/s13204-020-01382-2.
[45] Mallikarjunaswamy C, Lakshmi Ranganatha V, Ramu R, Udayabhanu, Nagaraju G. Facile microwave-assisted green synthesis of ZnO nanoparticles: application to photodegradation, antibacterial and antioxidant. J Mater Sci Mater Electron. 2020;31:1004–21. doi: 10.1007/s10854-019-02612-2.
[46] Anvarinezhad M, Javadi A, Jafarizadeh-Malmiri H. Green approach in fabrication of photocatalytic, antimicrobial, and antioxidant zinc oxide nanoparticles–hydrothermal synthesis using clove hydroalcoholic extract and optimization of the process. Green Process Synth. 2020;9(1):375–85. doi: 10.1515/gps-2020-0040.

Appendix

Table A1: FT-IR spectra with possible assignments

Frequency (cm^{-1})	Possible assignment	Functional group
S. acuta extract		
3,292.72	O–H stretch	Alcohol/phenol
2,924.88	C–H bend	Aliphatic
2,853.51		
1,727.68	CO–NH bend	Amide
1,609.34	N–H bend	Primary amines
1,440.22	C–C bend	Aromatic carbon
1,361.15	C–N stretch	Amide
1,236.42	C–N bend	Aliphatic amine
1,023.54		
827.45	–C═C–H stretch	Alkyne
Phyto-fabricated ZnO NPs		
544.12	Zn–O	Zinc oxide

Table A2: Antioxidant potentiality of phyto-fabricated ZnO NPs from *S. acuta*

Concentration ($mg \cdot mL^{-1}$)	ZnO NPs	Plant extract
0.2	31.88 ± 0.30^{c}	05.08 ± 0.10^{e}
0.4	38.37 ± 1.54^{c}	08.24 ± 0.20^{d}
0.6	45.95 ± 0.39^{bc}	14.42 ± 0.41^{c}
0.8	50.08 ± 1.14^{b}	21.42 ± 0.41^{b}
1	59.64 ± 2.58^{a}	25.43 ± 0.43^{a}

Values are the means of four independent replicates. ± indicate standard errors. Means followed by the same letter(s) within the same column are not significantly ($p \leq 0.05$) different according to Tukey's HSD.